BIAXIAL TENSILE TESTING

Development of a biaxial tensile testing machine and a nondisturbing displacement measurement method

JEAN-PHILIPPE URRUTY, RÉGNIER HUCHON, AND JEAN POUYET

ABSTRACT

A biaxial tensile machine is presented which describes the mechanical behavior of anisotropic sheet materials. Two servohydraulic actuators, controlling each other independently, impose a tensile stress on a cruciform flat specimen in two perpendicular directions. The sample design has been optimized to reach the highest possible isotropic biaxial strain field. The heterogeneous and anisotropic nature of fibrous materials, the ratifying of behavior laws, and the inadequacy of the usual techniques have led us to develop an optical method to measure in-plane displacements. This technique is based on real-time location of a grid of points by an image processing system composed of two CCD cameras and two video digitizers. Data are numerically stored to calculate the in-plane strain field of the tested material.

Classical uniaxial tests are suitable for the evaluation of mechanical properties of materials. However, for anisotropic sheet materials such as polymers, paper, paperboard, or tissue, biaxial stress tests are required to approximate real loading but are generally difficult to implement and to analyze. The problem lies in the fact that the identification of mechanical properties is related to both specimen design and loading system.

This paper presents a biaxial tensile testing machine developed in our laboratory, and applied to the characterization of the rheological behavior of various sheet materials. The mechanism uses two electrohydraulic actuators in a displacement control mode providing axial loads on a flat cruciform specimen.

Noncontacting and nondisturbing metrologies are required to identify in-plane displacement fields on materials that are subjected to large deformation under loading. Among nondestructive techniques, optical methods have the advantage of a minimum interaction with the structure, which avoids the possibility of local disruptions, and allows the measurement of the whole strain field as well as local measurement. Optical methods also allow studies in high strain gradient zones with high strain concentration or in areas with crack propagations. Nowadays, these techniques are more and more widely used for strain calculation, to observe plasticity or damage phenomena, and to determine material behavior.

This paper also describes a special optical setup to characterize samples surface displacement field.

BIAXIAL TESTING APPARATUS

Existing devices

One broadly used multiaxial test, the burst test *(1, 2)* is based on the application of a uniform pressure, normal to the face of a circular flat specimen gripped on its edge. This test presents such major drawbacks as difficulty in controlling the principal stress ratio, nonuniformity of stress and strain distributions, and tedious analysis.

Another test submits tubular specimens to axial load and/or axial torque, with or without applying external or internal pressure *(3, 4)*. While the principal stress ratio may be changed, shear stress may occur. Cylindrical geometries can yield false predictions of mechanical properties in the case of anisotropic films, especially when using pasted-up lap joints specimens.

One kind of test consists in in-plane loading along two perpendicular directions on a square or cruciform sample. This technique has been reported by several authors and seems to be the most appropriate for anisotropic sheet materials.

Boelher *et al. (5)* have reported the use of a screw-driven biaxial testing machine to stretch or to compress composite plates or rolled sheet metals on a vertical frame. The cruciform specimen geometry has been optimized and a new specific off-axes testing device makes the biaxial tensile tests more significant.

San Miguel *(6)* described a system aimed at propellant study, driven by two step-motors and equipped with a thickness transducer and a 70-mm camera. The square specimen is clamped by pins. Pictures of an engraved grid on the sheet are recorded at fixed time intervals.

Hardacker *(7)*, using an apparatus with four servomotors, has shown the presence of a central uniform stress zone despite the translation of the central part of the sample. The test equipment developed by Sakaguchi *(8)* is equipped with movable load-bearing bars driven by two servomotors. Seven chucks on each side are used to secure the square flat specimen.

The biaxial tensile testing machine presented by Makinde *et al. (9)* uses four hydraulic actuators and a new extensometer for composites or metallic materials. The problem with the load alignment system and the displacement of the central part of the sample were the reasons why they recommend the use of two independent hydraulic circuits.

Additional workers have reported on a static monotonic or creep biaxial apparatus for plane specimens *(10–13)*. Finally, the adaptation of a uniaxial tension machine to produce biaxial efforts is not effective *(14, 15)*.

Therefore, loads are applied either by electric or hydraulic motors. The latter, being easier to implement, allow the study of a larger choice of materials. In any case, the synchronization of all the functions was difficult to achieve with instruments providing four efforts. Those possessing only two actuators are more reliable and electronic regulation is easier; however, the installation of a clamp translation system is required *(16)*.

Specimen geometry

The lack of standards and the fact that the size and shape of a biaxial tension specimen are related to material and testing equipment, compels users to design their own sample. However, the cruciform specimen which satisfies biaxiality conditions *(17)* is the most accepted geometry. The rectangular form requires a more complex clamping system *(6)*.

Reinhardt *(18)* has reported a detailed experimental study of specimen shape and clamp system to initiate ruptures in the central zone. The machine is equipped with four clamps, moved by 10 pistons on each face. The strain field is obtained by photographic methods.

Moreover, in the case of large deformations, the slots in the cruciform specimen arms reduce lateral stiffness and optimize strain field homogeneity in the equibiaxial strain field.

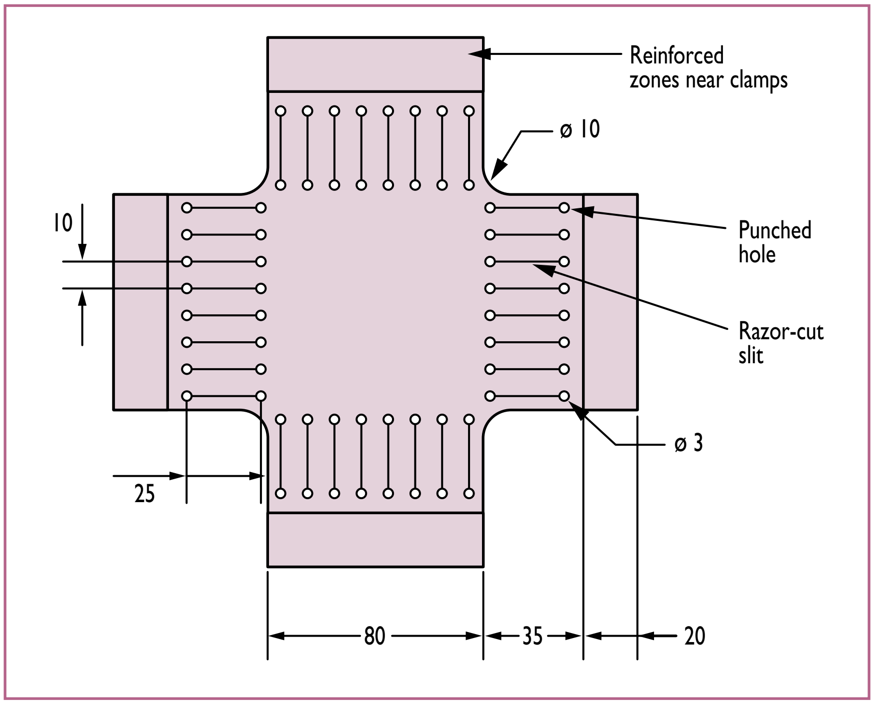

1. Cruciform specimen design (dimensions in millimeters)

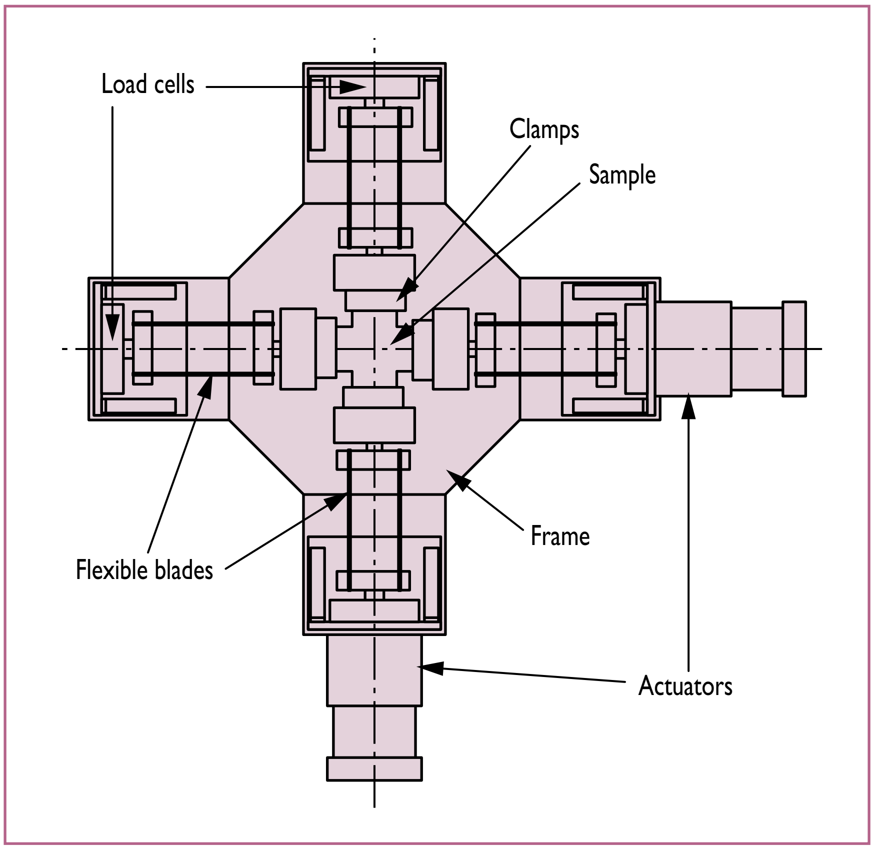

2. Plane side of the biaxial tensile test machine

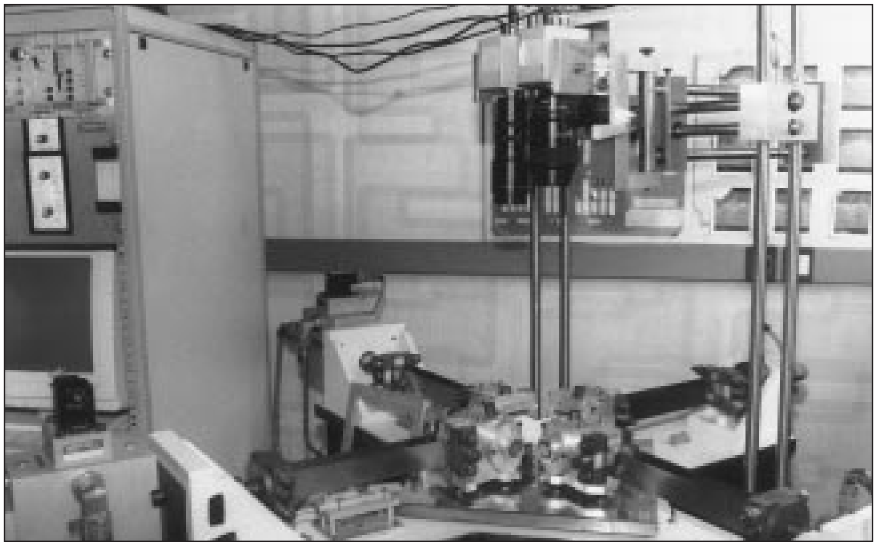

3. Photograph of the biaxial tensile test machine

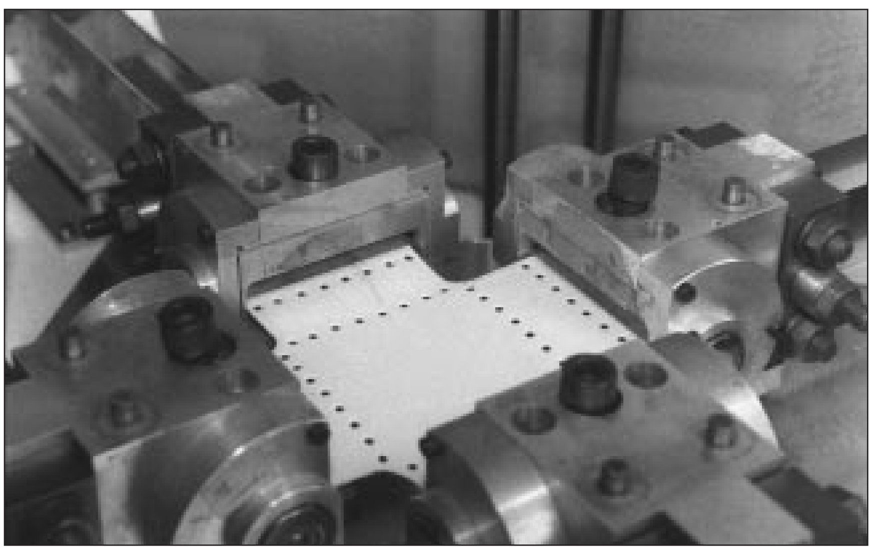

4. Photograph of clamp system and vision system

The existence of stress concentrations in the joining zones causes premature ruptures. Shear stresses always exist regardless of specimen shape or the stress nature.

The uniform biaxial strain state is determined via stress minimization in the sample central zone and consequently through a particular design. This geometry can be evaluated by the finite elements method *(19)*. As a first approximation, the material is assumed to be homogeneous, isotropic and in a plane stress state. In the resultant configuration, shown in **Fig. 1**, the uniform biaxial strain zone covers a 30-mm diameter circular central area. This specimen design is similar to different authors' choice *(9)*. It has also been found to be suitable for biaxially loaded precracked sheet studies *(20)*.

Apparatus characteristics

The suggested apparatus has been conceived according to the sample design previously described. As depicted in **Figs. 2 and 3**, the horizontal position of the cruciform rigid frame eases a right disposition of all mechanical elements. The frame, subjected to high bending stresses under load, is constituted of steel slabs (thickness: 30 mm). Its dimensions are overdesigned to reduce unavoidable strains. The measured maximum deflection is less than 0.04 mm at the frame center.

Axial loads are generated by two linear servo-electrohydraulic actuators in the range of 0-10 kN. They are transmitted through each arm with two thin flexible steel blades (0.56 mm), with low bending stiffness, to the clamps supported by ball bearings. The sample holding is made through two removable files linked with clamps. These files can rotate around a horizontal axis by a guide sleeve and allow a right plane position of the sample **(Fig. 4)**. The alignment and positioning of all machine components was done by optical sighting.

This device is either load- or displacement-controlled. The two actuators work independently, so that different principal stress ratios are possible. Each of the two channels possesses its own control system consisting of a ramp generator, a servovalve, a servocontroller and a linear-variable differential transformer (LVDT). This latter has a stroke of 60 mm and a precision of more than 0.1% full scale. The displacement control mode uses the comparison of the command signal transmitted to the servovalve and the response signal delivered by the LVDT transducer.

The hydraulic circuit includes servovalves, servoactuators and a 1.5 L/min 15-MPa pump. Fluid temperature is controlled by an air-cooled heat-exchanger.

The axial load is measured by two removable flat load cells which are positioned on the static clamp.

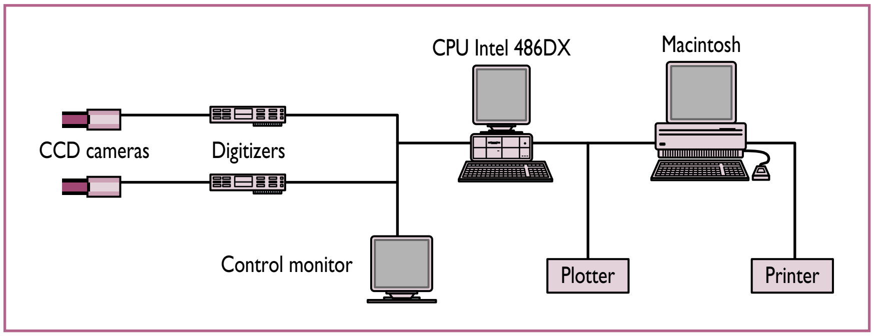

5. Strain analysis setup

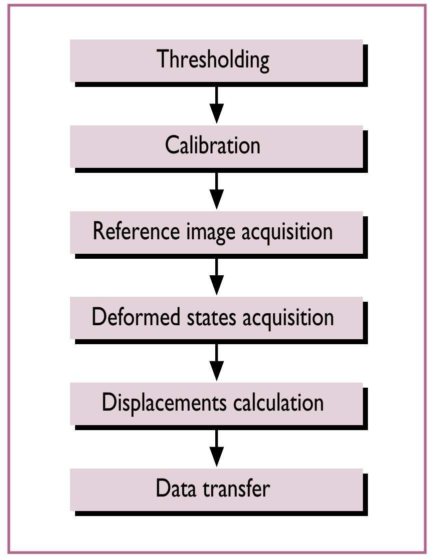

6. Displacements evaluation flow

Output signals from load and displacement transducers are transferred to a personal computer through a 12-bit analog-digital interface.

An optical extensometer was also used in uniaxial tensile tests to correlate the displacement of marks disposed onto the sample with the extension between the clamped zones. The loading system deformations, being 20 times lower than specimen strains, are assumed to be insignificant. The circular isotropic biaxial strain state in the central part of the sample was confirmed by a photoelastic study of polycarbonate plates and by strain gauge measurements on aluminum *(19)*.

Stress evaluation

The complex problem of stress distribution, especially in heterogeneous materials, leads us to seek a suitable kind of metrology. Indeed, it is difficult to evaluate an equivalent surface. When the sample can be molded or machined and has a thinner central area, it is possible to evaluate an equivalent section in the case of an isotropic material and for a given strain path *(15)*.

The problem is really more complex in the case of an anisotropic material with uniform thickness. Dubroca carried out uniaxial tensile tests on aluminum alloy, PVC, and kraft paper to calculate the elastic constants (Young's modulus, Poisson ratios) *(19)* in order to determine an efficient surface by comparison of uniaxial and biaxial states of stress. This value depends on the mechanical properties and the geometrical design of the sample, as well as strain rate.

The several problems that appear—for example, the impossibility to evaluate the stress field, the heterogeneous nature of some materials, the ratifying of the behavior laws, and the inadequacy of the usual techniques—led us to consider the means to identify the displacement and strain fields on surface of the sample [see Ref. *(21)*].

STRAIN MEASUREMENT

Extensometers or strain gauges are not really suitable for the study of strain fields in sheet materials, such as tissues, polymers or papers. For instance, gluing effects associated with strain gauges alter the measurements of mechanical properties.

Among optical methods, the interferometric ones, such as holographic interferometry *(22, 23)*, speckle *(24)*, and moire *(25-27)* have been developed for various applications. Their accuracy is good but equipment stability requirements and data processing are laborious and time consuming.

Digital image processing systems are used in many applications *(28-32)*, but show some drawbacks: a lot of data to store images, low speed of image acquisitions, difficulty to record operations and numerical treatments, and the high cost of high spatial resolution systems.

Nevertheless, this kind of image processing system seems appropriate to identify the displacement field over the specimen. Besides its optical method advantages, the chosen setup is suitable for the mechanical biaxial device, and is rather easy to implement.

Displacements evaluation

The experimental setup shown in **Fig. 5** is composed of two CCD video cameras, two A/D converters in a host personal computer, a video controller, and a separate computer for data analysis. It allows the tracking, during the mechanical tests, of round black grid dots marked on the samples' white surfaces. These dots, four at least, are 0.1-mm diameter and are printed or preferably deposited by letter transferring.

Each camera (752 x 582 photosensitive elements) is synchronized with the other one and delivers fully interlaced monochromatic television pictures (625 lines/50 Hz). To improve spatial accuracy, two vision systems (camera and video digitizer) are coupled and are focused on different regions of the specimen. The

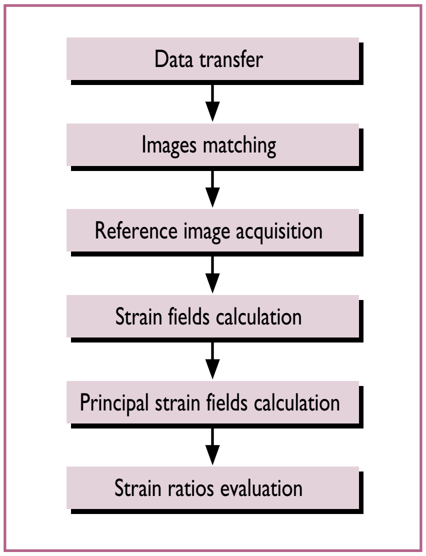

7. Strains evaluation flow

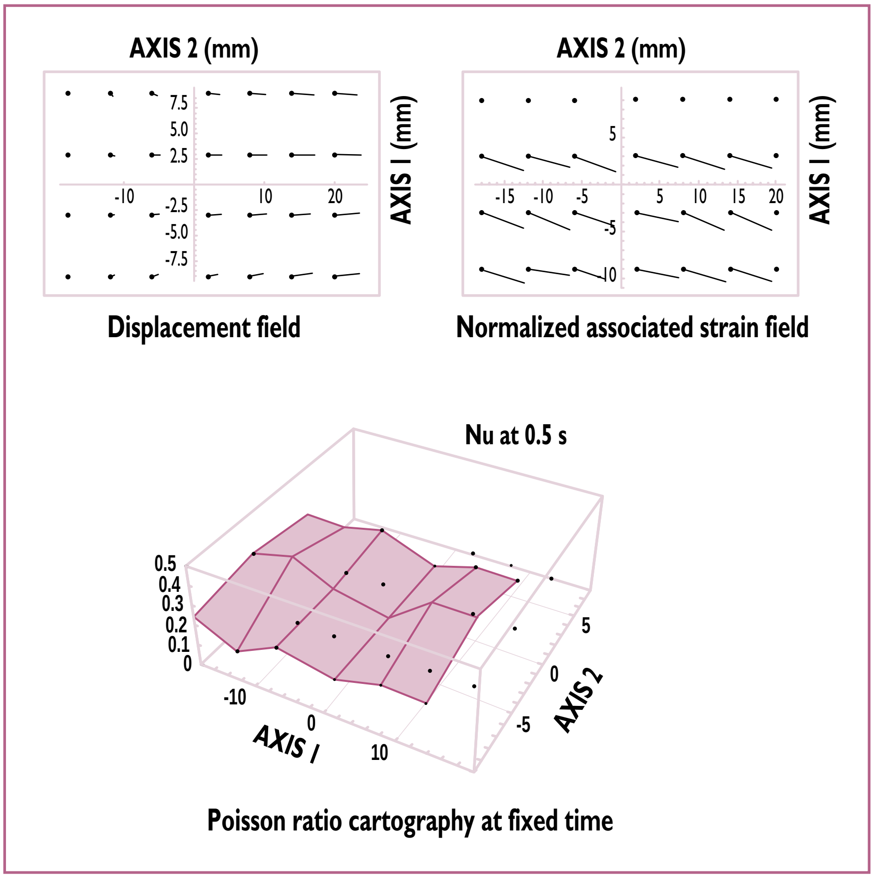

8. Results of the uniaxial tensile test simulation

threshold is obtained from the image histogram. Acquisition operations such as sampling, quantifying, coding, but also image compression, are made by the digitizer itself in 512 x 512-pixel formats. During the whole test, data transfer in computer memory is done in "real-time," i.e., faster than the frame scanning period (40 ms). The location of the center of each grid point is calculated with a centroid algorithm *(33)* and compared to a reference frame, which corresponds to a small prestrained state, to yield the displacement field. Then, storage on disk can be carried out. This instrumentation allows a high-performance acquisition rate, faster than the classical systems *(29)*.

Optical calibration consists of evaluating two parameters in order to convert any distance into an image to the associated real distance on the specimen. These parameters depend on various factors such as lens magnification, pixel dimensions, light illumination, thresholding, and digitizers resolution. Practically, they are calculated with a well-known circular target *(34)*.

The distance between the optic axes of cameras can be modified either with a specific optical device adaptator or mechanically in order to change the measurement scale.

The development of this strain evaluation technique required the creation of two programs for data acquisition and numerical treatment, respectively. The aim of the former is mainly to determine various positions of each grid point during the mechanical test, frame after frame. It consists of several procedures compiled by C++ that execute the operations described in **Fig. 6.** This software manages the connections with the digitizers such as threshold writing, frame memory reading or calibration. The data are then transferred through two files that contain the frame reference point positions and all the point displacements in each local system. A second program has been developed from a macro-language to perform, successively, image matching, strain field and strain ratios calculations as described in **Fig. 7** and developed in the following section.

Strain field analysis

The aim of this section is to calculate the strain field in the specimen plane according to measured displacements. We used the Lagrangian approach of media continuum mechanics, which consists in comparing the configuration of body *(S)* at time t to its reference configuration S_o at time t_o *(35)*. The motion of each solid element is observed by the transformation of its spatial and temporal coordinates and leads to the use of the right Cauchy-Green tensor $\overline{\overline{C}}$, also called dilatation's tensor in Lagrangian formulation, and the Green-Lagrange strain tensor $\overline{\overline{E}}$ between S_o and S states.

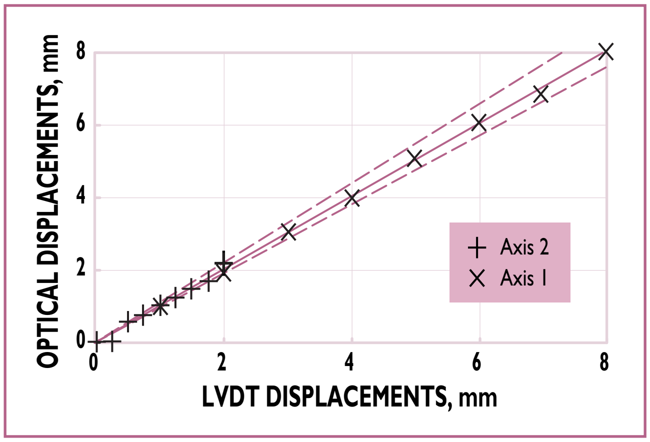

9. Simulation: comparison between real and measured displacements

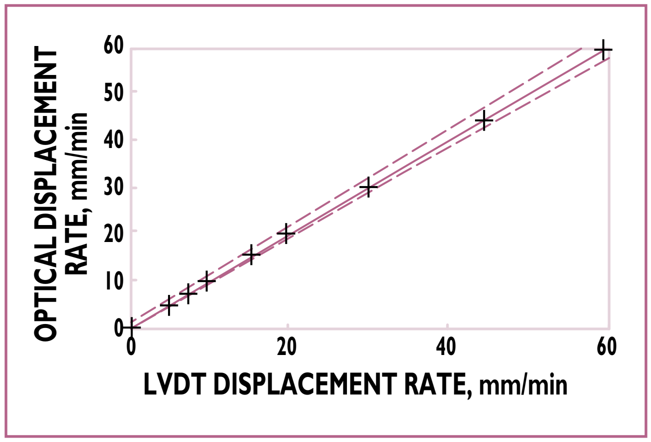

10. Rigid-body motion results

KEYWORDS

Anisotropy, audio visual aids, bibliographies, cameras, computers, displacement, instrumentation, optical instruments, loads, mechanical properties, optical instruments, rheological properties, simulation, strain gauges, strain properties, strains, stress, tensile tests, test equipment, test methods.

$$\bar{\bar{E}} = 1/2(\bar{\bar{C}} - \bar{\bar{I}}) \qquad (1)$$

Only the in-plane displacements being considered, u_i^j and v_i^j, denote the two displacement vector components at point (i, j).

With discretization by first-order progressive finite difference (36), the strain tensor components at time t in the 1-2 references axis, can be written as follows:

[SEE PAGE 289 FOR EQ. 2]

where the initial distances between two points, respectively, in 1 and 2 directions are $\Delta L_{i,i+a}$ and $\Delta L_{,j,j+ß}$, a taking values between 1 and n_1–1, ß between 1 and n_2 1 for a n_1 x n_2 points grid.

The principal strains are related by well-known equations.

Baseline tests

Tests have been performed to verify the accuracy of the method. They consist of two methods: strain field simulations and real time rigid body motions measurements.

In the first test, calculations carried out during data analysis proceeds as follows. Files similar to those issued from real acquisition are generated. They represent the displacements of a grid of points subjected to basic loading (translation along one direction, uniaxial tension or compression…). Results from a numerical simulation corresponding to a uniaxial tensile test on a 7 x 4-grid of points are presented in **Fig. 8.** It was verified that the algorithm is independent of rigid-body motions and the obtained results, e.g., strains and Poisson ratios, correspond to the expected ones, only numerical errors exist in this case.

The second test consists in using different grids with various pitches to simulate deformable solids extensions. A grid with well-defined position dots is placed under the 1 optical system and acquisition is made through the described device. Data analysis allows comparison of measured displacements with theoretical values **(Fig. 9)**. The displacement error is lower than the expected value of 0.07 mm for magnification factors that equal 0.040 mm/pixels (horizontal direction) and 0.054 mm/pixels (vertical direction).

Time-based translations of an aluminum plate with grid points are produced through the movable clamp of the tensile test machine. The measurement is carried out in two different ways: the first one through the method described above, the second through a linear position transducer (LVDT). We note in **Fig. 10** that although small differences are measured for each image, the results are in accordance with LVDT data and the error margin is as expected.

CONCLUSIONS

A mechanical testing machine has been developed to apply tensile loads according to two orthogonal directions on a flat cruciform specimen. This apparatus has been conceived to predict the rheological behavior of various sheet materials and particularly anisotropic materials such as paper, paperboard, tissue, and polymers. A cruciform design sample is suggested in order to optimize the central isotropic strain area.

Furthermore, a new optical method to identify in-plane displacements is suggested. The location of a grid points is made in real time through two video acquisition systems that are composed each of a CCD camera and a video digitizer. This technique provides the dis-

$$\left[\varepsilon_{11}\right]_{i,i+\alpha}^{j} = \frac{1}{2}\left\{ \frac{2\left(u_{i+\alpha}^{j} - u_{i}^{j}\right)}{\Delta L_{i,i+\alpha}} + \left(\frac{u_{i+\alpha}^{j} - u_{i}^{j}}{\Delta L_{i,i+\alpha}}\right)^{2} + \left(\frac{v_{i+\alpha}^{j} - v_{i}^{j}}{\Delta L_{i,i+\alpha}}\right)^{2} \right\}$$

$$\left[\varepsilon_{22}\right]_{i}^{j,j+\beta} = \frac{1}{2}\left\{ \frac{2\left(v_{i}^{j+\beta} - v_{i}^{j}\right)}{\Delta L_{j,j+\beta}} + \left(\frac{u_{i}^{j+\beta} - u_{i}^{j}}{\Delta L_{j,j+\beta}}\right)^{2} + \left(\frac{v_{i}^{j+\beta} - v_{i}^{j}}{\Delta L_{j,j+\beta}}\right)^{2} \right\}$$

$$\left[\varepsilon_{12}\right]_{i,i+\alpha}^{j,j+\beta} = \frac{1}{2}\left\{ \frac{u_{i}^{j+\beta} - u_{i}^{j}}{\Delta L_{j,j+\beta}}\left(1 + \frac{u_{i+\alpha}^{j} - u_{i}^{j}}{\Delta L_{i,i+\alpha}}\right) + \frac{v_{i+\alpha}^{j} - v_{i}^{j}}{\Delta L_{i,i+\alpha}}\left(1 + \frac{v_{i}^{j+\beta} - v_{i}^{j}}{\Delta L_{j,j+\beta}}\right) \right\} \quad (2)$$

placement of each point, at standard video frequency, with the expected precision. This last point will be improved in the future with the development of CCD array and digitizer resolutions.

The investigations in progress consist of tension tests on the mentioned films to determine in-plane elastic constants, and especially the less well known Poisson ratios. The results will provide a more equivalent description for the mechanical behavior of anisotropic sheets under multiaxial loading, both in the equibiaxial strain field, central to the cruciform specimen, and near the crack tip in the case of pre-cracked samples. **TJ**

Urruty is a postdoctoral fellow, Huchon is associate professor, and Pouyet is professor at Laboratoire de Mécanique Physique, Université Bordeaux I, 351 Cours de la Libération, 33405 Talence, France.*

The authors wish to thank warmly Smurfit Worldwide Research Europe for the support provided for mechanical devices.

Received for review Jan. 3, 1995.

Accepted June 16, 1995.

* Now postdoctoral researcher at University Laval and College FX-Garneau.

LITERATURE CITED

1. Suhling, J. C., *1987 International Paper Physics Conference Proceedings,* TS CPPA, Montreal, p. 139.
2. Dudderar, T. D., Koch, F. B., and Doerries, E. M., *Exp. Mech.* 17(4): 133(1977).
3. Duggan, M. F. and Bailie, J. A., *Proceedings 1980 International Conference on Composite Materials,* Paris, p. 900.
4. De Ruvo, A., Carlsson, L. and Fellers, C., *Tappi* 63(5): 133(1980)
5. Boelher, J. P., Demmeerle, S., and Koss, S., *Exp. Mech.* 34 (1): 1(1994).
6. San Miguel, A., *Exp. Mech.* 12(3): 155(1972).
7. Hardacker, K.W., *J. Phys. Sci. Instr.* 14: 593(1981).
8. Sakaguchi, K., Kawabata, S., Kawai, H., *et al., J. Soc. Mat. Sci. Japan* 17(175): 356(1967).
9. Makinde, A., Thibodeau, L., and Neale, K. W., *Exp. Mech.* 32(2): 138(1992).
10. Charvat, I.M.H. and Garrett, G. G., *J. Test. Eval.* 8(1): 9(1980).
11. Fessler, H. and Musson, J. K., *J. Strain Anal.* (1): 22(1969).
12. Parsons, M. W. and Pascoe, K. J., *J. Strain Anal.* 10(1): 1(1975).
13. Radon, J. C., Leevers, P. S., and Culver, L. E., *Exp. Mech.* 17(6): 228(1977).
14. Arenz, R. J., Landel, R. F., and Tsuge, K., *Exp. Mech.* 15(3): 114(1975).
15. Makinde A., Ph.D. thesis, Université de Poitiers, 1986.
16. Chaudonneret, M., Gilles, P., Labourdette, R., *et al., La Recherche Aerospatiale* 5: 299(1977).
17. Monch, E. and Galster, D., *Brit J. Appl Phys.* 14: 810(1963).
18. Reinhardt, H., *Exp. Mech.* 16(2): 71(1976).
19. Dubroca, S., Ph.D. thesis, Université Bordeaux I, 1984.
20. Huchon, R. and Pouyet J., *Proceedings of 1989 Conference,* Groupe Français de Rheologie, Paris, p. 900.
21. Brémand, F. and Lagarde, A., *Arch. Mech.* 40(5–6): 515(1988).
22. Françon, M., "L'optique moderne depuis l'apparition du laser," Hachette, Paris, 1986.
23. Olofsson, K., Molin, N. E., and Kyosti, A., *Tappi J.* 74 (3): 195(1991).
24. Castagnède, B. and Mark, R. E., *C. R. Acad. Sci. Paris* 305(2): 221(1987).
25. Dadkhah, M. S., Wang, F. X., and Kobayashi, A.S., *Exp. Tech.* 12(7):28 (1988).
26. Di Chirico, G., Ginesu, F., and Rossi, R., *Exp. Mech.* 29(12): 420(1989).
27. Han, B. and Post, D., *Exp. Tech.* 13(7): 25(1989).
28. Bremand, F., Dupre, J. C., and Lagarde, A., *Eur. J. Mech., A/Solids* 11: 349(1992).
29. Sutton, M.A. and Chao, Y. J., *Tappi J.* 70(3): 173(1988).
30. Choi, D., Thorpe, J. L., and Hanna, R. B., *Wood Sci. Technol.* 25: 251(1991).
31. G'sell, C., Hiver, J.M., Dahoun A., *et al., J. Mat. Sci.* 27: 5031(1992).
32. Sirkis, J. S. and Lim, T. J., *Exp. Mech.* 31(12): 382(1991).
33. Miyoshi, A., Yoshioka, A., and Yagawwa, G., *Eng. Comput.* 3: 149(1988).
34. Belaid, A., *Proceedings of the 1990 International Conference on Pattern Recognition,* Atlantic City, NJ, p. 636.
35. Germain, P. "Cours de mécanique des milieux continu," Masson, Paris, 1973.
36. Sibony, M. and Mardon, J.C., "Approximations et équations différentielle," Hermann, Paris, 1984.